Chemical Engineering Journal 161 (2010) 1–8

Contents lists available at ScienceDirect

Chemical Engineering Journal

journal homepage: www.elsevier.com/locate/cej

Biosorption of aluminum ions onto *Rhodococcus opacus* from wastewaters

Javier Enrique Basurco Cayllahua, Maurício Leonardo Torem*

Department of Materials Engineering, Pontifical Catholic University of Rio de Janeiro, 225, Marquês de São Vicente Street, Rio de Janeiro, Brazil

ARTICLE INFO

Article history:
Received 15 September 2009
Received in revised form 8 March 2010
Accepted 16 March 2010

Keywords:
Biosorption
Aluminum
Wastewaters
Rhodococcus opacus

ABSTRACT

This fundamental work deals with the biosorption removal of Al (III) using a *Rhodococcus opacus* strain. Several variables that have an effect on the capacity of aluminum biosorption from water streams by *R. opacus* were studied, particularly the effects of solution pH, biosorbent concentration, metal concentration, contact time, ionic strength and temperature of biosorption. The most favorable biosorption pH value of Al (III) was determinate as around 5.0 and the maximum sorption capacity was found to be 41.59 mg g^{-1} at pH 5.0 (initial concentration of 50 mg L^{-1}) and temperature 25 °C.

The experimental data obtained have been analyzed using four two-parameter models (Langmuir, Freundlich, Temkin and Dubinin-Radushkevich) and two three-parameter models (Redlich–Peterson and Sips). In order to determine the best fit isotherm, three error analysis methods were used to evaluate the data: correlation coefficient, chi-square and residual root mean square error. Dynamics of sorption process were studied and the values of rate constant of biosorption were calculated. The uptake capacity is a function of pH solution, ionic strength and biosorbent concentration.

1. Introduction

Metals are known to be essential for all living organisms. Nevertheless, when the concentrations exceed certain limits, the metals can become toxic and harmful to them. The presence of low concentrations of aluminum ions in water streams can reach the food chain and produce a variety of neurological and skeletal disorders in humans. For this reason, the environmental pollution control authorities have imposed a tight control on the discharge of wastewater containing heavy metals from industries to watercourses [1]. Precipitation, ion exchange, adsorption, membrane technology and reduction methods are employed for metal treatment and recovery [2].

On the other hand, heavy metals' biosorption is a promising procedure for the treatment of wastewaters containing metallic species by using wastes from agricultural and industrial activities, seaweed and specially propagated biomasses of bacteria, yeast and fungi as alternative sorbent materials [3,4]. The literature shows few works related to the biosorption of light metals such as aluminum [5–8].

Investigation of the physicochemical mechanisms involved in metal removal (such as physical adsorption, ion exchange, surface complexation and surface micro-precipitation) is a fundamental step for the optimization of the operating conditions, product development and process design [9].

The aim of this research was to study the biosorption mechanism of Al (III) onto *Rhodococcus opacus* strain and contribute to a better understanding and modeling of the equilibrium and dynamic processes. The sorption capacity of Al (III) was evaluated by varying experimental conditions, viz. solution pH, biosorbent concentration, ionic strength, contact time and temperature. Furthermore the *R. opacus* was characterized by Fourier transformer infrared spectroscopy (FTIR) and Zeta potential. The experimental data were correlated to different kinetic and isotherm models and the corresponding parameters were determined.

2. Materials and methods

2.1. Bacteria and media

R. opacus obtained from the culture collection of the Tropical Foundation of Researches and Technology André Tosello (SP, Brazil), was used in this study. The bacterium was grown in a liquid media containing: 3 g L^{-1} malt extract, 3 g L^{-1} yeast extract, 5 g L^{-1} peptone and 10 g L^{-1} glucose at 28 °C under agitation at 175 rpm. All the products used in a medium were from Vetec (RJ, Brazil). The medium was sterilized by autoclaving at a pressure 1 atm. The pH of the grown medium was adjusted to 7.2 by the addition of 1 M KOH. After the bacterial cells' growth, the culture was separated by centrifugation at 2000 × *g* for 25 min. The cell pellet was washed with deionized water and suspended in NaCl 0.1 mM and later being sterilized at 1 atm of pressure during 20 min. The quantification of the biomass concentration was determined by dry weight.

---

* Corresponding author. Tel.: +55 21 3527 1723; fax: +55 21 3527 1236.
E-mail address: torem@puc-rio.br (M.L. Torem).

1385-8947/$ – see front matter © 2010 Elsevier B.V. All rights reserved.
doi:10.1016/j.cej.2010.03.025

2.2. Electrokinetic measurements

The zeta potential curves of *R. opacus* were built up, at different pH values in order to determine its isoelectric point and the influence of the presence of 10^{-4} mol L^{-1} of Al (III). The measurements were realized with a zeta meter (Zeta Meter System 3.0+). The suspension, consisting of cells and Al (III), was placed in the electrophoresis cell, and a molybdenum rod-type anode and a platinum strip-type cathode were inserted into the opposite ends of the cell and connected to the Zeta Meter power unit. The zeta potential was determinate with a stereoscopic microscope over a distance of 160 μm with a direct current of know voltage.

2.3. Batch biosorption studies

The effect of the wastewater pH solution on the Al (III) sorption capacity of *R. opacus* cells was studied varying the pH from 3.0 to 6.0, using a metal solution concentration of 50 mg L^{-1}. The final concentrations of the solutions were measured by flame atomic absorption spectrophotometer.

All biosorption experiments were carried out in a single run basis. The Al (III) solutions were prepared by dissolving of $AlCl_3 \cdot 6H_2O$ analytical grade in deionized water Vetec (RJ, Brazil). Experiments were conducted in 125 mL Erlenmeyer flasks containing known concentration of Al (III). Flasks were agitated on a shaker at 175 rpm for 8 h to ensure that the equilibrium was reached. Samples (20 mL) were taken for the determination of residual concentration. The metal biosorption capacity was determinate at different initial metal concentrations. The effect of temperature on biosorption equilibrium was studied by shifting temperatures from 25 to 45 °C. Effect of biosorbent concentration on uptake capacity of Al (III) was investigated by increasing the *R. opacus* concentration from 2.0 to 5.0 g L^{-1} with an initial Al (III) concentration of 40 mg L^{-1}. The amount of metal adsorbed was calculated using the equation (1):

$$q_e = \frac{(C_0 - C_e) \times V}{M} \tag{1}$$

where C_0 and C_e are the initial and equilibrium concentrations of aluminum (III) (mg L^{-1}), M the dry weight of *R. opacus* biomass (g) and V is the volume of solution (L). Apart from the regression coefficient (R^2), chi-square (χ^2) and the residual root mean square error (RMSE) were used to measure the goodness-of-fit [10].

2.4. Equilibrium modeling

The sorption equilibrium data are conveniently represented by sorption isotherms, which correspond to the relationship between the mass of the solute sorbed per unit mass of sorbent q_e and the solute concentration for the solution at equilibrium C_e. The biosorption isotherms were investigated using six equilibrium models, which are namely the Langmuir, Freundlich, Temkin, Dubinin-Radushkevich, Redlich–Peterson and Sips isotherm models were analyzed.

The Langmuir equation describes the adsorption of gas molecules on a planar surface [11].

$$q_e = \frac{q_m b C_e}{1 + b C_e} \tag{2}$$

where q_e is the amount adsorbed at equilibrium (mg g^{-1}), and b is a constant related to the affinity of the binding sites, q_m is the maximum adsorption capacity (mg g^{-1}). The empirical Freundlich model can be applied to non-ideal adsorption on heterogeneous surfaces as well as multilayer adsorption and is expressed by the following equation [12]:

$$q_e = K_F C_e^{1/n} \tag{3}$$

K_F and n are equilibrium constants indicative of adsorption capacity and adsorption intensity, respectively. The Temkin isotherm assumes that the fall in the heat of adsorption is linear rather than logarithmic, as implied in the Freundlich model [13]:

$$q_e = \frac{RT}{b} \ln(A C_e) \tag{4}$$

where R is the gas constant, T the absolute temperature in Kelvin, b the constant related to the heat of adsorption and A is the Temkin isotherm constant.

Dubinin [14] developed the following isotherm in accounting for the effect of the porous structure of an adsorbent:

$$q_e = q_{DR} \exp(-\beta F^2) \tag{5}$$

where q_{DR} is the Dubinin-Radushkevich constant representing the theoretical monolayer saturation capacity [15], β is the constant of the adsorption energy (kJ^2 mol^{-2}) which is related to mean adsorption energy E; and F is the Polanyi potential and is defined by:

$$F = RT \ln\left(1 + \frac{1}{C_e}\right) \tag{6}$$

$$E = \frac{1}{\sqrt{2\beta}} \tag{7}$$

The mean adsorption energy E gives information about chemical and physical adsorption [16].

Redlich and Peterson [17] incorporated the features of the Langmuir and Freundlich isotherms into a single equation and presented a general isotherm equation.

$$q_e = \frac{K_{RP} C_e}{1 + a_{RP} C_e^{\beta_{RP}}} \tag{8}$$

Where K_{RP} is the Redlich–Peterson model isotherm constant (L g^{-1}), a_{RP} the Redlich–Peterson model constant (L mg^{-1}), β_{RP} the Redlich–Peterson model exponent. The exponent, β_{RP}, lies between 0 and 1. There are two limiting behaviors: Langmuir form for $\beta = 1$ and Henry's law form $\beta = 0$.

Sips [18] proposed an empirical isotherm equation, also kwon as Langmuir–Freundlich isotherm, which is often expressed as:

$$q_e = \frac{K_s C_e^{ns}}{1 + a_s C_e^{ns}} \tag{9}$$

where K_S is the Sips constant (L mg^{-1}), a_S is the affinity coefficient (L mg^{-1}) and ns is the heterogeneity coefficient. At low sorbate concentrations it effectively reduces to a Freundlich isotherm and thus does not obey Henry's law. At high sorbate concentrations, it predicts a monolayer adsorption capacity characteristic of the Langmuir isotherm.

2.5. Kinetic studies

Kinetic studies were carried out at constant pH around 5 with initial concentration (50 mg L^{-1}) and adsorbent concentration of 2 g L^{-1} at various temperatures (25, 35 and 45 °C). The samples were withdrawn at suitable time intervals, centrifuged and then analyzed for Al (III) residual concentrations.

2.6. Fourier transformer infrared spectroscopy

Infrared absorption spectra were recorded on a Nicolet FTIR 2000 spectrophotometer; a KBr matrix was used as reference and a deuterated triglycine sulfate (DTGS) as detector. The data acquisition was carried out through the absorption mode. The *R. opacus*

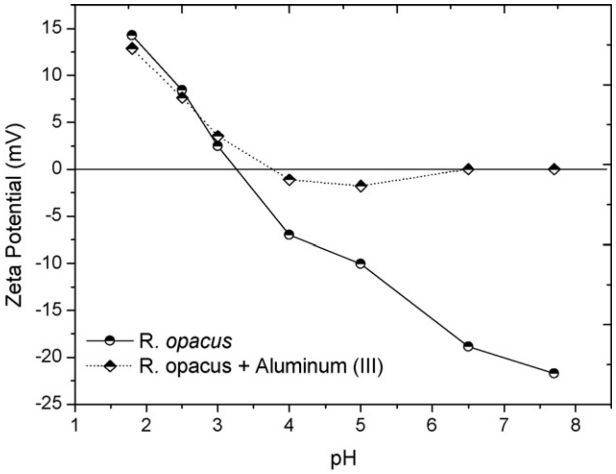

Fig. 1. Zeta potential of *R. opacus* in 1 mM NaCl (a neutral electrolyte) and aluminum solutions (C_0: 10 mg L^{-1}, biosorbent concentration: 50 mg L^{-1}, and agitation time: 20 min).

cell suspension with and without aluminum samples were filtered and dried at 70 °C. The dried powder was properly mixed in a KBr matrix. The spectra were collected after 120 scans at 4 cm^{-1}.

3. Results and discussion

3.1. Zeta potential measurements

All bacterial cells are covered by a cell wall which can be composed of peptidoglycan, (lipo-) polysaccharides, (lipo-) proteins and enzymes. These macromolecules have shown the presence of carboxyl, sulfate, phosphate and amino functional groups. The presence of anionic and cationic groups conferred the amphoteric behavior to the cell wall. Studies by Van Der Wal et al. [19] have shown that anionic groups dominate over cationic groups.

This seems to be a general phenomenon and it is in agreement with the observation that most bacterial cells have isoelectric points below pH 4.0. As observed in this work, the isoelectric point of the bacteria *R. opacus*, in the presence of an indifferent electrolyte, 1 mM NaCl, was 3.26. The *R. opacus* was net negatively charged at pH values above his isoelectric point.

Fig. 1 shows the zeta potential curve for *R. opacus*, before and after interaction with aluminum metal ions. A change is observed in the surface properties of *R. opacus* after interaction with the aluminum metal ions. The isoelectric point was shifted to pH value around 3.75. One can attribute the shift in the isoelectric point value to a specific adsorption of Al (III) onto *R. opacus* cells [20].

3.2. Effect of solution pH

It is well recognized that the pH of the aqueous solution is an important parameter in affecting biosorption of heavy metal ions [21]. Nevertheless, it should be stressed that there are very few works regarding the use of *R. opacus* as a biosorbent for metals uptake [22–24]. Biosorption of Al (III) onto *R. opacus* as a function of pH was studied and the results are shown in Fig. 2. With pH increasing, Al (III) uptake increased quickly from 3.0 to 5.0 and then increased slowly at pH above of 6. Similar works were carried out for the biosorption of Cu, Pb, and Cr [25,26] and Cd and Zn [27].

The effect of pH can be explained both in terms of pH_{IEP} (isoelectric point) of the biosorbent or acidic nature (pK_a) and concentration of the active sites present on cell wall. At $pH < pH_{IEP}$, the surface charge of the biosorbent is positive due to be closely associated with the hydronium ions (H_3O^+) and restricted the approach of metal cations as a result of repulsive force. On the other hand, when $pH > pH_{IEP}$, the surface of biosorbent is negatively charged, thereby it is easily for the positively charged Al (III) to be adsorbed. The electrostatic attraction may play an important role in the biosorption of negatively charged metal ions by the biosorbents [28]. For pH values greater than the pK_a, the sites are mainly in dissociated form and can exchange H^+ with metal in solution. The percentage removal of Al (III) ion was obtained by calculation using the following equation:

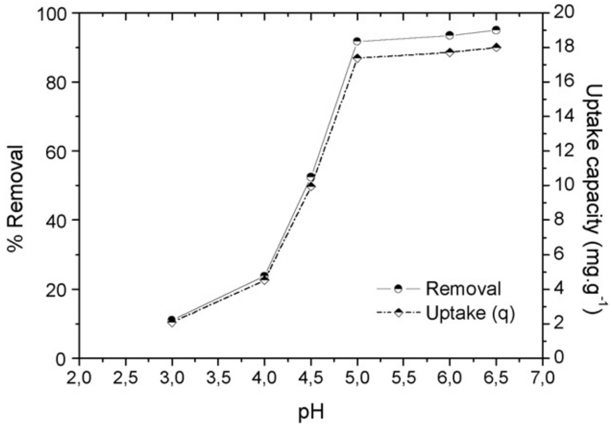

Fig. 2. Effect of solution pH on Al (III) uptake onto *R. opacus* (biosorbent dose: 2 g L^{-1}; initial concentration: 50 mg L^{-1}; T = 298 K).

$$\text{Removal}(\%) = \frac{C_i - C_e}{C_i} \times 100 \tag{10}$$

C_i and C_e (mg L^{-1}) are the initial concentration an equilibrium concentration, respectively. At pH 3, the maximum Al (III) removal efficiency was only 11%, whereas at pH 4.5 the removal efficiency increased to 52%. The better value for aluminum ions' removal was found at pH 5 where the maximum removal was 92%; these results are in good accordance to [29,30]. Thus, all the biosorption experiments were conducted at this optimum pH value.

3.3. Effect of biosorbent concentration

To determine the effect of biosorbent concentration, different amounts of *R. opacus* were placed in contact in 50 mL of solution in which the concentration of Al (III) was 40 mg L^{-1} (under optimized conditions of pH). The extent of removal and sorption capacity of Al (III) onto bacteria strain are shown in Fig. 3. The removal efficiency, decreased from 92% to 75.53% with increase in biosorbent concentration from 2.0 to 5.0 g L^{-1}. In the same profile was observed for the equilibrium adsorption capacity, q_e, decreased from 21.88 to 7.21 mg g^{-1}. A similar trend for the biosorption removal of nickel onto peat was also reported [31]. However the decrease in the uptake capacity with an increase in biosorbent concentration could be related by the interaction of the self functional groups present in the cell wall of *R. opacus*.

These results are in good accordance to those obtained by Bueno et al. [25] and Vasquez et al. [27] which point out that the effect of the biomass concentration is deeply related to the metal species, its concentration in solution and the contact time for the uptake step.

3.4. Adsorption isotherms

The equilibrium adsorption isotherms for the biosorption of aluminum onto *R. opacus* were measurement at several temperatures and a controlled solution pH of 5. The measured data with correlation coefficients for several studied models are given in Table 1. From the two-parameter isotherm, the Temkin model is best suit-

Table 1
Isotherm model constants for the biosorption of Al (III) onto *R. opacus*.

	Temperature						
		q_m (mg g^{-1})	b (L mg^{-1})		R^2	RMSE	χ^2
Langmuir constants	298	41.584	0.961		0.995	0.8182	0.6695
	308	34.488	0.399		0.973	1.535	2.356
	318	37.081	0.235		0.976	2.049	1.432
		K_F (L g^{-1})	n		R^2	RMSE	χ^2
Freundlich constants	298	19.158	2676		0965	2.121	4.493
	308	11.704	2.789		0.963	1.806	3.262
	318	9.527	2.406		0.959	1.869	3.493
		A (L mol^{-1})	b_T		R^2	RMSE	χ^2
Temkin constants	298	287.13	7.705		0.997	0.022	0.0005
	308	123.49	9.720		0.984	0.043	0.0019
	318	65.23	8.887		0.978	0.051	0.0026
		q_{DR} (mmol g^{-1})	β (mmol^2 kJ^{-2})		R^2	RMSE	χ^2
Dubinin-Radushkevich constants	298	1.651	0.012		0.996	0.025	0.0007
	308	1.225	0.016		0.975	0.055	0.003
	318	1.239	0.021		0.973	0.057	0.003
		K_{RP} (L g^{-1})	a_{RP} (L mg^{-1})	β_{RP}	R^2	RMSE	χ^2
Redlich–Peterson constants	298	49.575	1.452	0.899	0.998	0.617	0.381
	308	21.766	1.025	0.834	0.983	1.372	1.884
	318	11.107	0.449	0.870	0.978	1.513	2.288
		K_s (L g^{-1})	a_s (L mg^{-1})	ns	R^2	RMSE	χ^2
Sips constants	298	36.177	0.797	0.865	0.997	0.724	0.524
	308	14.283	0.341	0.742	0.980	1.467	2.152
	318	9.413	0.226	0.857	0.978	1.542	2.378

able for describing the biosorption equilibrium of Al (III) onto *R. opacus*. The Temkin isotherm plot for Al (III) at different temperatures is given in Fig. 4.

From Table 1 it is observed that q_m parameter from the Langmuir isotherm decreases with increasing temperatures, what it wants to say that as to increase the temperature the maximum uptake capacity decreases. A dissimilar trend was also reported for the aluminum biosorption onto brown algae [32]. A great value of b parameter implied strong bonding of Al (III) to *R. opacus* at several temperatures.

Conversely, the n parameter from the Freundlich isotherm was greater than unity at various temperatures indicating a favorable adsorption process [33].

From the Dubinin-Radushkevich isotherm the value determined for E was 15.04 kJ mol^{-1}, which is within the 8–16 kJ mol^{-1} range for chemical adsorption. Consequently, it is reasonable to suggest that a fraction of the All (III) biosorption onto *R. opacus* probably can be related to a specific interaction (chemical bonding) [34].

In contrast, Redlich–Peterson, three-parameter isotherm, is the best model to fit the experimental data in the studied concentration range. The Redlich–Peterson isotherm plot for Al (III) at several temperatures is given in Fig. 5. From Table 1 it is worth noting that β_{RP} values were close to unity, i.e., the data can preferably be fitted with Langmuir model.

The values of K_S parameter from Sips isotherm increased with increasing temperatures. This model confirms the heterogeneity of the biosorbent surface since $0 < \text{ns} < 1$ at various temperatures. On the other hand, Table 2 presents the comparison of biosorption

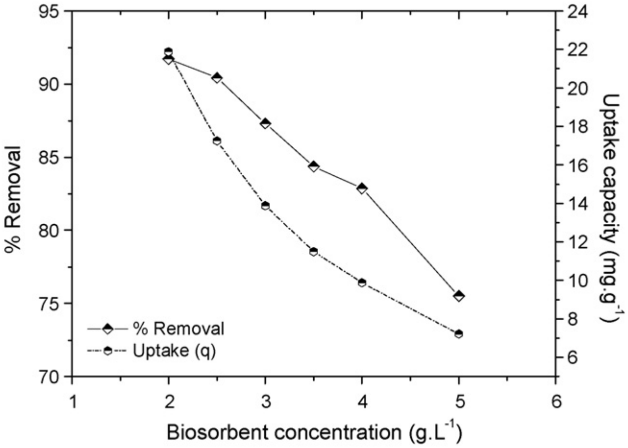

Fig. 3. Effect of biosorbent concentration on Al (III) uptake onto *R. opacus* (equilibrium solution pH: 5; initial concentration: 50 mg L^{-1}; biosorbent dose: 2 g L^{-1}; T = 298 K).

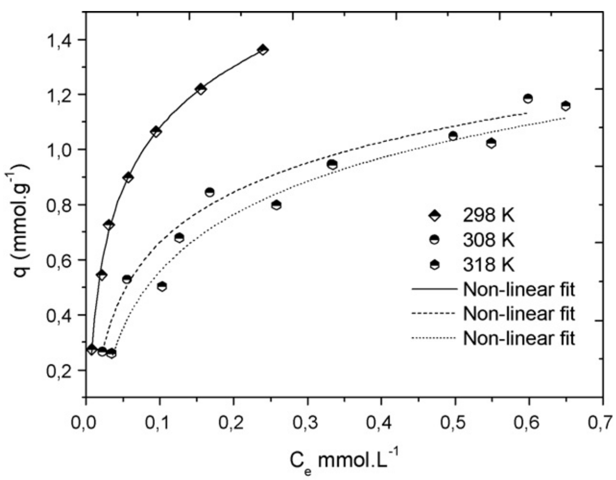

Fig. 4. Temkin isotherm of Al (III) onto *R. opacus* at several temperatures.

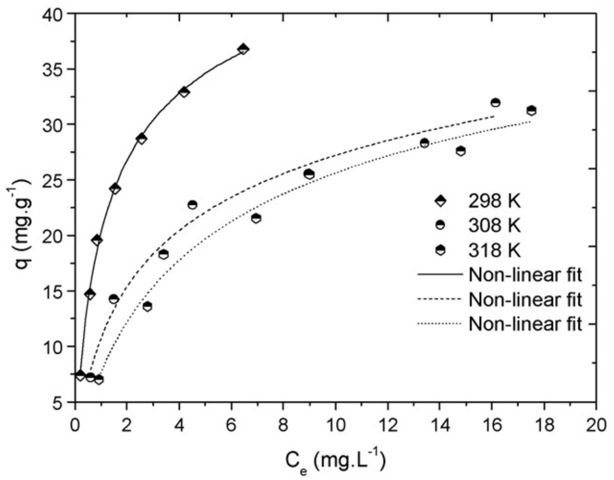

Fig. 5. Redlich–Peterson isotherm of Al (III) onto *R. opacus* at several temperatures.

Table 2
Comparison of sorption capacity of *R. opacus* Al(III) with that of different biosorbents.

Biosorbent	Sorption capacity (mg g^{-1})	pH	Reference
Chryseomonas luteola TEM05	55.2	5.0	[33]
Typha domingensis leaf powder	0.35	2.5	[38]
BDH activated carbon	6.56	4.0	[39]
Padina pavonica	77.30	4.5	[40]
Rhodococcus opacus	41.59	5.0	Present study

capacity of *R. opacus* for aluminum with that of various biosorbents reported in the literature [30,35–37].

3.5. Determination of equilibrium time

Equilibrium time is a function of many factors, such as type of biosorbent (number and kind of functional groups), size and form of biosorbent, physiological state of biomass, as well as the metal involved in the biosorption system [38]. The distribution of sorbate between biosorbent and solution is influenced by agitation time. The effect of contact time on biosorption at various temperatures was studied between 0 and 180 min. The results are presented in Fig. 6. In general, a two-stage kinetic behavior is observed: rapid initial biosorption in a contact time of 5 min, followed by a second stage with a poor biosorption rate.

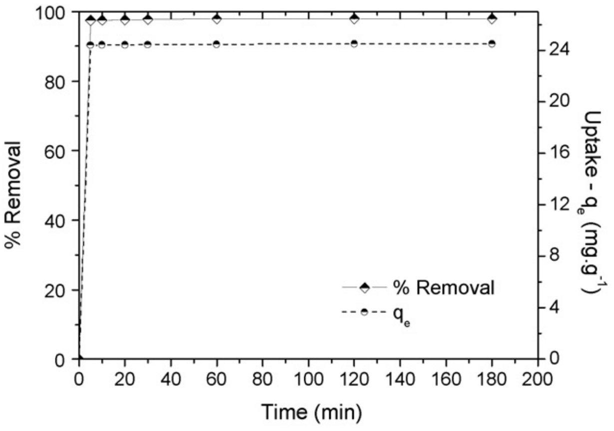

Fig. 6. Aluminum (III) biosorption against time (biosorbent dose: 2 g L^{-1}; initial concentration: 50 mg L^{-1}; pH 5; T = 298 K).

3.6. Kinetic studies

There have been several reports [39] on the use of different kinetic models to describe the experimental data of biosorption. In order to investigate the mechanism of biosorption, the following kinetic models are generally used to test experimental data. The pseudo-first-order rate Lagergren model [40]

$$\frac{dq_t}{dt} = k_{1,\mathrm{ad}}(q_\mathrm{e} - q_t) \tag{11}$$

where q_e and q_t are the amounts of metal ions adsorbed onto biosorbent (mg g^{-1}) at equilibrium and at time t, respectively; $k_{1,\mathrm{ad}}$ is the rate constant of first-order (min^{-1}). After integration between boundary conditions (t = 0 to t and q_t = 0 to q_e), Eq. (11) becomes:

$$q_t = q_\mathrm{e}[1 - \exp(-k_{1,\mathrm{ad}}t)] \tag{12}$$

The pseudo-second-order model [41] is based on the sorption capacity of the solid phase and is expressed as:

$$\frac{dq_t}{dt} = k_{2,\mathrm{ad}}(q_\mathrm{e} - q_t)^2 \tag{13}$$

where $k_{2,\mathrm{ad}}$ is the rate constant of second-order biosorption (g mg^{-1} min^{-1}), q_e the amount of metal ions adsorbed at equilibrium (mg g^{-1}) and q_t the amount of solute sorbate on the surface of the biosorbent at any time t (mg g^{-1}) [42]. For boundary conditions (t = 0 to t and q_t = 0 to q_e), Eq. (13) becomes Eq. (14), and is the integrated rate law for a pseudo-second-order reaction.

$$q_t = \frac{q_\mathrm{e}^2 k_{2,\mathrm{ad}}}{1 + q_\mathrm{e} k_{2,\mathrm{ad}} t} \tag{14}$$

The intraparticle-diffusion model [43] is characterized by a linear relationship between the amount adsorbed, q_t, and the square root of the time and is expressed as:

$$q_t = k_p t^{0.5} + C \tag{15}$$

where q_t the amount of the metal ions adsorbed at time t (mg g^{-1}) and k_ip is the initial rate of intraparticle diffusion (mg L^{-1} s$^{-0.5}$).

The applicability of the three models mentioned above was checked by fitting of the experimental data by the appropriate equations (Fig. 7(a)–(c)). Table 3 lists the results obtained from experimental data, which indicate that the pseudo-second-order kinetic equation provided the best model for describing the biosorption of the Al (III) onto *R. opacus*.

The Boyd equation was also applied to check that sorption proceeds via external diffusion or intraparticle-diffusion mechanism [44]. The equation can be expressed in the following form:

$$X = \left(1 - \frac{6}{\pi^2}\right)\exp(-\mathrm{Bt}) \tag{16}$$

where $X = q_t/q_\mathrm{e}$ and Bt is a mathematical function of F which can be calculated from each value of F as:

$$\mathrm{Bt} = -0.4977\ln(1 - X) \tag{17}$$

Plots of Bt versus t are shown in Fig. 7(d), which are straight lines. The linearity of these plots is employed to distinguish between external-transport (film diffusion) and intraparticle-transport controlled rates of biosorption [45].

A straight line passing through the origin is indicative of biosorption process governed by particle-diffusion mechanisms; otherwise they are governed by film diffusion [44]. From Fig. 7(d) the plot was neither linear nor passed through the origin. This could indicate that film diffusion is the rate-limiting biosorption process for Al (III). However, further studies are required to establish the

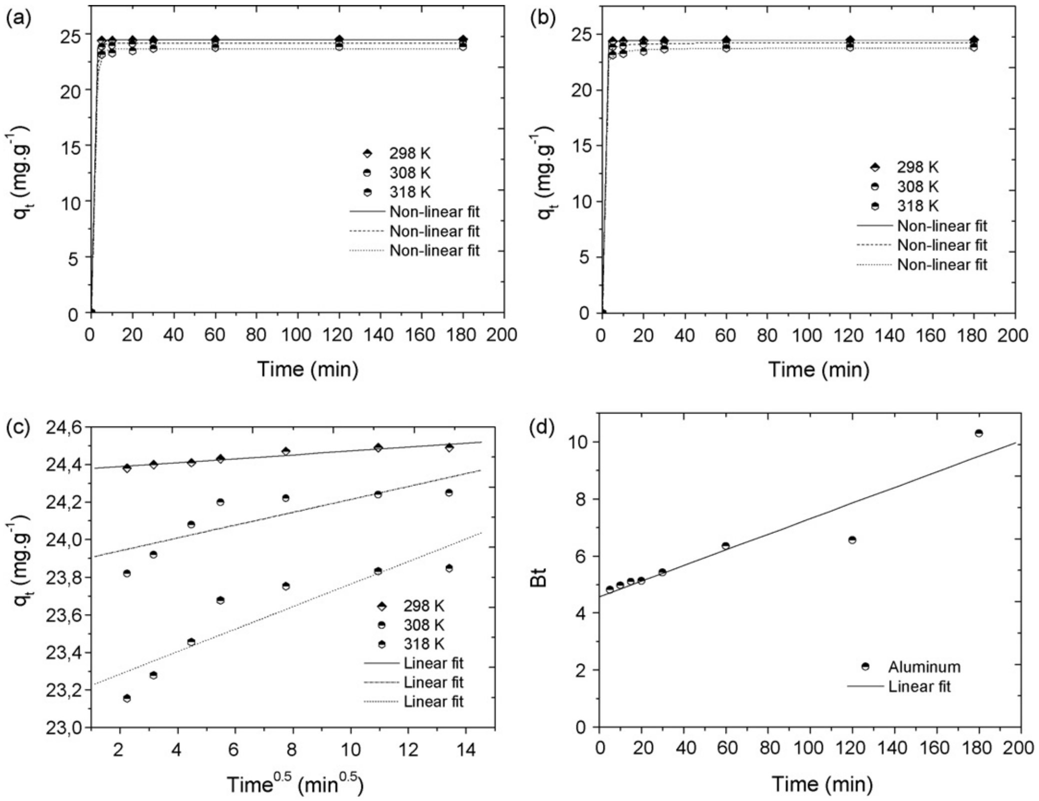

Fig. 7. Kinetic models: (a) pseudo-first-order model, (b) pseudo-second-order model and (c) intraparticle-diffusion model (d) Boy's plot, for biosorption of Al (III) onto *R. opacus*.

Table 3
Kinetic parameters for the biosorption of Al (III) onto *R. opacus*.

Temperature (K)	k_1 (min^{-1})	R_1^2	k_2 (g mg^{-1} min^{-1})	R_2^2	k_{ip} (mg g^{-1} min$^{-0.5}$)	R_s^2
298	1.175	0.9992	1.828	0.9999	0.0104	0.957
308	0.853	0.9991	0.416	0.9999	0.0342	0.826
318	0.769	0.9991	0.263	0.9999	0.0599	0.896

same. The effective diffusion coefficient (D_i) was calculated using the following relation [46]:

$$B_b = \frac{\pi^2 D_i}{r_0^2} \tag{18}$$

Here B_b is calculated from the slope of Bt versus time plot, D_i (cm^2 s^{-1}) is the effective diffusion coefficient of Al (III) in the sorbent and r_0 is the average radius of sorbent particles assumed to be spherical. According to Singh et al. [47], a D_i value in the order of 10^{-11} cm^2 s^{-1} is indicative of intraparticle diffusion as rate-limiting step. In this study the value of Di for the *R. opacus* loaded with Al (III), obtained were in the order of 1.11×10^{-10} cm^2 s^{-1}, which was more than one order of magnitude higher, indicating that the intraparticle diffusion was no the rate-controlling step.

3.7. Fourier transformer infrared (FTIR) studies

The FTIR spectra of unloaded and metal loaded *R. opacus* biomass in the range of 500-4000 cm^{-1} were taken to confirm the presence of functional groups that are usually responsible for the biosorption process and are presented in Fig. 8. Studies developed by Volesky [48] and Pavan et al. [49] concluded that the main functional groups responsible for a biosorption process are the hydroxyl, carbonyl, carboxyl, sulfonate, amide, imidazole, phosphate and phosphodiester groups, some of them present on the *R. opacus*. Table 4 shows an absorbance bands and the characteristic functional groups of *R. opacus*.

In Fig. 8 one can observe the displacement of the vibration band from 3414 to 3378 cm^{-1} pertaining to hydroxyl group. The

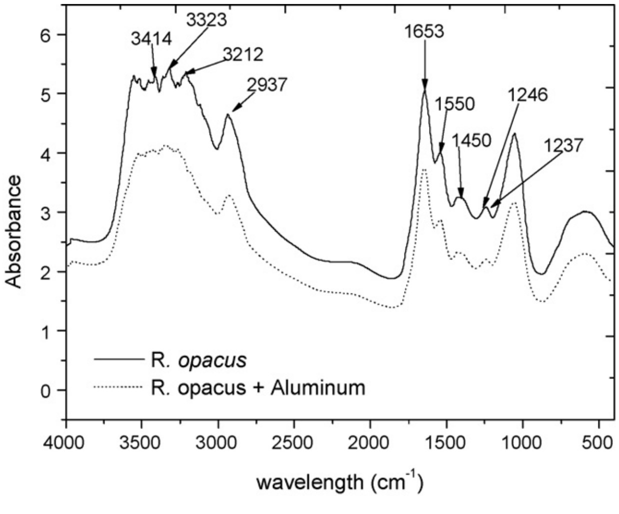

Fig. 8. FTIR spectra for *R. opacus* before and after Al (II) interaction (biosorbent dose: 2 g L^{-1}; initial concentration: 50 mg L^{-1}; pH 5; T = 298 K).

Table 4
Absorbance bands and the characteristic functional groups of *R. opacus*.

Wavelength (cm^{-1})	Functional group
3500–3200	N–H or O–H stretching
3200–2800	Alkyl hydrocarbon
2962, 2872; 2926, 2855	Asymmetric and symmetric stretching of CH_3 and CH_2
1750–1620	C=O stretching
1460–1455	CH_3 and CH_2 bending
1250–1220	Symmetric stretching of PO_2^- P=O alongamento simétrico do PO_2^-
1075–1000; 1150–1075; 1210–1100	Alcoholic stretching C–O
~720	C–CH_2 rocking

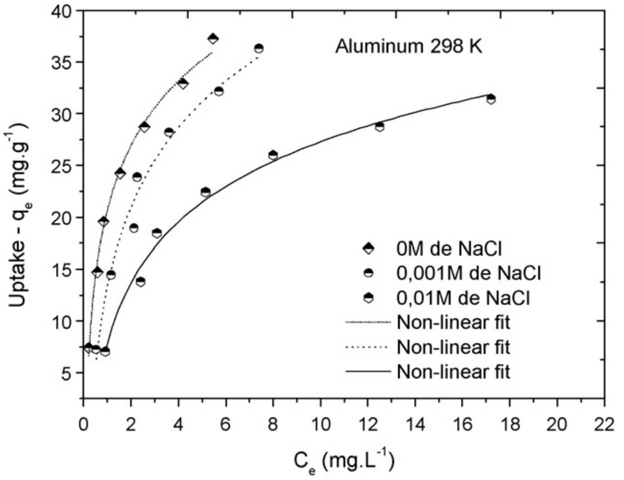

Fig. 9. Effect of ionic strength on the Al (III) biosorption (biosorbent dose: 2 $g\,L^{-1}$; initial concentration: 50 $mg\,L^{-1}$; T = 298 K).

amino group was whom demonstrated further interaction to the aluminum ions, displacement of the vibration band from 3323 and 3212 cm^{-1} to 3305 cm^{-1} and 3183 cm^{-1}. The carbonyl, carboxyl and phosphate group present little displacement in theirs vibration bands. These changes of the spectra clearly show the complexation/coordination of the metal ions during the biosorption process. However, it is difficult to explain the exact mechanism of the biosorption of metal ions onto *R. opacus* due to unidentified peaks.

3.8. *Effect of ionic strength*

Ionic strength has a key impact on the uptake of the Al (III) onto *R. opacus* (Fig. 9). In the presence of 0.01 and 0.1 M NaCl, the maximum uptake capacities (q_m) of the Al (III) ions were decreased with the increase in the ionic strength. This can be explained in terms of two aspects. Firstly, competition of Na+ ions with the Al (III) ions for sorption sites of *R. opacus* resulted in the observed decrease in the maximum uptake capacities with increasing electrolyte NaCl concentration. Secondly, adsorption is sensitive to the change in ionic strength if electrostatic attraction is a significant mechanism. Thus the results show that electrostatic attraction plays an important role in the adsorption of Al (III) ions onto *R. opacus*. At high ionic strength, the increased amount of NaCl can help to swamp the surface of the biosorbent, which decrease aluminum ions access to the surface active sites. When biosorbent is in contact with sorbate species in solution, they are bound to be surrounded by an electrical diffused double layer, the thickness of which is significantly expanded by the presence of electrolyte. Such expansion inhibits the biosorbent particles and Al (III) ions from approaching each other more closely and, through the decreased electrostatic attraction, results in the decreased uptake of Al (III) ions.

4. Conclusion

Biosorption performances of *R. opacus* are studied in terms of kinetic and biosorption isotherms for the removal of Al (III) from aqueous solutions. The kinetic experiments show that the biosorption is rapid and maximum uptake capacity achieved in 20 min. Kinetic models evaluated included the pseudo-first, pseudo-second-order model, intraparticle diffusion and Boy's equation. The kinetic data were well fitted by pseudo-second-order model due to their high regression coefficient and low chi-square and RMSE values. Equilibrium isotherm data were fitted using different two-parameter model, Temkin model is in good agreement with the experimental data. In the case of the three-parameter model, the Redlich–Peterson model was found to provide closest fit to the experimental data. It was noted that a decrease in temperature, biosorbent concentration and ionic strength resulted in a higher aluminum loading per unit weight of the biosorbent. The biosorption of Al (III) ions onto *R. opacus* was found to be pH dependent and the higher removal was found a pH around 5.

Acknowledgements

The authors would like to acknowledge the financial support given by FAPERJ, CNPq and CAPES.

References

[1] D. Kratochvil, B. Volesky, Advances in the biosorption of heavy metals, Trends in Biotechnology 16 (1998) 291–300.
[2] T.A. Kurniawan, G.Y.S. Chan, W.H. Lo, S. Babel, Physico-chemical treatment techniques for wastewater laden with heavy metals, Chemical Engineering Journal 118 (2006) 83–98.
[3] F. Vegliò, F. Beolchini, Removal of metals by biosorption: a review, Hydrometallurgy 44 (1997) 301–316.
[4] J. Wase, C. Forster, Biosorbents for Metal Ions, Taylor & Francis Ltd, London, 1997.
[5] T.L. Macdonald, R.B. Martin, Aluminum ion in biological systems, Trends in Biochemical Science 13 (1988) 15–19.
[6] N.D. Priest, The biological behavior and bioavailability of aluminium in man, with special reference to studies employing aluminium-26 as a tracer: review and study update, Journal of Environmental Monitoring 6 (2004) 375–403.
[7] I Narin, M. Tüzen, M. Soylak, Aluminium determination in environmental samples by graphite furnace atomic absorption spectrometry after solid phase extraction on amberlite XAD-1180/pyrocatechol violet chelating resin, Talanta 63 (2004) 411–418.
[8] M. Tuzen, M. Soylak, Biosorption of aluminum on pseudomonas aeruginosa loaded on chromosorb 106 prior to its graphite furnace atomic absorption spectrometric determination, Journal of Hazardous Materials 154 (2008) 519–525.
[9] B. Volesky, Sorption and Biosorption, Bv Sorbex, Canada, 2003.
[10] Y.S. Ho, J.F. Porter, G. Mckay, Equilibrium isotherm studies for the biosorption of divalent metal ions onto peat: copper, nickel and lead single component systems, Water Air Soil Pollution 141 (2002) 1–33.
[11] I. Langmuir, The constitution and fundamental properties of solids and liquids, Journal of the American Chemical Society 38 (1916) 2221–2295.
[12] H.M.F. Freundlich, Over the adsorption in solution, Journal Physical Chemistry 57 (1906) 385–470.
[13] C. Aharoni, M. Ungarish, Kinetics of activated chemisorption. Part 2. Theoretical models, Journal of Chemical Society Faraday Transaction 73 (1977) 456–464.
[14] M.M. Dubinin, The potential theory of adsorption of gases and vapors for adsorbents with energetically non-uniform surface, Chemical Review 60 (1960) 235–266.
[15] C.A. Başar, Applicability of the various adsorption models of three dyes adsorption onto activated carbon prepared waste apricot, Journal of Hazardous Materials B15 (2006) 232–241.
[16] W. Riemam, H. Walton, Ion Exchange in Analytical Chemistry, Pergamon Press, Oxford, 1970.
[17] O. Redlich, D.L. Peterson, A useful adsorption isotherm, Journal of Physical Chemistry 63 (1959) 1024.
[18] R. Sips, Combined form of Langmuir and Freundlich equations, Journal of Chemical Physics 16 (1948) 490–495.
[19] A. Van Der Wal, W. Norde, A.J.B. Zehnder, J. Lyklema, Determination of total charge in the cell walls of gram-positive bacteria, Journal of Colloids and Surface. B, Biointerfaces 9 (1997) 81–100.

[20] J. Lyklema, Adsorption of small ions, in: G.D. Parfitt, C.H. Rochester (Eds.), Adsorption from Solution at the Solid/Liquid Interface, Academic Press, London, 1983, pp. 223–246.

[21] H. Hasar, Adsorption of nickel (II) from aqueous solution onto activated carbon prepared from almond husk, Journal of Hazardous Materials 93 (2003) 49–57.

[22] J. Febrianto, A.N. Kosasih, J. Sunarso, Y. Ju, N. Indraswati, S. Ismadji, Equilibrium and kinetic studies in adsorption of heavy metals using biosorbent: a summary of recent studies, Journal of Hazardous Materials 162 (2009) 616–645.

[23] G.M. Gadd, Biosorption: critical review of scientific rationale, environmental importance and significance for pollution treatment, Journal of Chemical Technology and Biotechnology 84 (2008) 13–28.

[24] P.T.M Ghazvini, S.G. Mashkani, Screening of bacterial cells for biosorption of oxyanions: application of micro-PIXE for measurement of biosorption, Hydrometallurgy 96 (2009) 246–252.

[25] B.Y.M. Bueno, M.L. Torem, F. Molina, L.M.S. de Mesquita, Biosorption of lead (II), chromium (III) and copper (II) by *R. opacus*: equilibrium and kinetic studies, Minerals Engineering 21 (2008) 65–75.

[26] B.A Calfa, M.L. Torem, On the fundamentals of Cr(III) removal from liquid streams by a bacterial strain, Minerals Engineering 21 (2008) 48–54.

[27] T.G.P. Vasquez, A.E.C. Botero, L.M.S. de Mesquita, M.L. Torem, Biosorptive removal of Cd and Zn from liquid streams with a *Rhodococcus opacus* strain, Minerals Engineering 20 (2007) 939–944.

[28] P.X. Sheng, L.H. Tan, J.P. Chen, Y.P. Ting, Biosorption performance of two brown marine algae for removal of chromium and cadmium, Journal of Dispersion Science and Technology 25 (2004) 679–686.

[29] D.G. Cetinkaya, Z. Aksu, A. Ozturk, T. Kutsal, A comparative study on heavy metal adsorption characteristics of some algae, Process Biochemistry 24 (1999) 885–892.

[30] G. Ozdemir, S.H. Baysal, Chromium and aluminum biosorption on *Chryseomonas luteola* TEM05, Applied Microbiology and Biotechnology 64 (2004) 225–232.

[31] Y.S. Ho, D.A.J. Wase, C.F. Forster, Batch nickel removal from aqueous solution by sphagnum moss peat, Water Resource 29 (1995) 1327–1332.

[32] A. Sari, M. Tuzen, Equilibrium, thermodynamic and kinetic studies on aluminum biosorption from aqueous solution by brown algae (*Padina pavonica*) biomass, Journal of Hazardous Materials (2009) 50–57.

[33] M.A.H Hanif, R. Nadeem, H.N. Bhatti, N.R. Ahmad, T.M. Ansari, Ni(II) biosorption by Cassia fistula (Golden Shower) biomass, Journal of Hazardous Materials B139 (2007) 345–355.

[34] E. Oguz, Adsorption characteristics and the kinetics of the Cr (VI) on the Thuja orientalis, Colloids and Surfaces A 252 (2005) 121–128.

[35] N.T. Abdel – Ghani, A.K. Hegazy, G.A. El-Chaghaby, Typha domingensis leaf powder for decontamination of aluminum, iron, zinc and lead: biosorption kinetics and equilibrium modeling, International Journal of Environmental Science and Technology 6 (2009) 243–248.

[36] S.A Al-Muhtaseb, M.H. El-Naas, S. Abdallah, Removal of aluminum from aqueous solutions by adsorption on date-pit and BDH activated carbons, Journal of Hazardous Materials 158 (2008) 300–307.

[37] A. Sari, M. Tuzen, Equilibrium, thermodynamic and kinetic studies on aluminum biosorption from aqueous solution by brown algae (Padina pavonica) biomass, Journal of Hazardous Materials 171 (2009) 973–979.

[38] A.R Khan, R.J. Ataullah, Equilibrium adsorption studies of some aromatic pollutants from dilute aqueous solutions on activated carbon at different temperatures, Journal of Colloid and Interface Science 194 (1997) 154–165.

[39] V. Padmavathy, P. Vasudevan, S.C. Dhingra, Adsorption of nickel(II) ions on Baker's yeast, Process Biochemistry 38 (2003) 1389–1395.

[40] S. Basha, Z.V.P. Murthy, Kinetic and equilibrium models for biosorption of Cr(VI) on chemically modified seaweed Cystoseira indica, Process Biochemistry 42 (2007) 1521–1529.

[41] Y.S. Ho, G. Mckay, Pseudo-second order model for sorption processes, Process Biochemistry 34 (1999) 451–465.

[42] I. Mohammad, El-Khaiary, Kinetics and mechanism of adsorption of methylene blue from aqueous solution by nitric-acid treated water-hyacinth, Journal of Hazardous Materials 147 (2007) 28–36.

[43] L. Lv, G. Tsoi, X.S. Zhao, Uptake equilibrium and mechanism of heavy metal ions on microporous titanosilicate ETS-10, Industrial and Engineering Chemistry Research 43 (2004) 7900–7906.

[44] G.E. Boyd, A.W. Adamson, L.S. Myers, The exchange adsorption of ions from aqueous solutions by organic zeolites. II. Kinetics, Journal of the American Chemical Society 69 (1947) 2836–2848.

[45] X.S. Wang, Y. Qin, Z.F. Li, Biosorption of zinc from aqueous solutions by rice bran: kinetics and equilibrium studies, Separation Science of Technology 41 (2006) 747–756.

[46] D. Mohan, K.P. Singh, Single- and multi-component adsorption of cadmium and zinc using activated carbon derived from bagasse—an agricultural waste, Water Research 36 (2002) 2304–2318.

[47] K.K. Singh, R. Rastogi, S.H. Hasan, Removal of Cr(VI) from wastewater using rice bran, Journal of Colloid and Interface Science 290 (2005) 61–68.

[48] B. Volesky, Biosorption and me, Water Research 41 (2007) 4017–4029.

[49] F.A. Pavan, A.C. Mazzocato, R.A. Jacques, S.L.P. Dias, Ponkan peel: a potential biosorbent for removal of Pb (II) ions from aqueous solution, Biochemical Engineering Journal 40 (2008) 357–362.